BIOCHEMISTRY
including biophysical chemistry & molecular biology

Article

pubs.acs.org/biochemistry

The Rate-Limiting Step of O_2 Activation in the α-Ketoglutarate Oxygenase Factor Inhibiting Hypoxia Inducible Factor

John A. Hangasky,[†] Hasand Gandhi,[‡] Meaghan A. Valliere,[†] Nathaniel E. Ostrom,[‡] and Michael J. Knapp*[,†]

[†]Department of Chemistry, University of Massachusetts, Amherst, Massachusetts 01003, United States

[‡]Department of Zoology, Michigan State University, East Lansing, Michigan 48824, United States

Supporting Information

ABSTRACT: Factor inhibiting HIF (FIH) is a cellular O_2-sensing enzyme, which hydroxylates the hypoxia inducible factor-1α. Previously reported inverse solvent kinetic isotope effects indicated that FIH limits its overall turnover through an O_2 activation step (Hangasky, J. A., Saban, E., and Knapp, M. J. (2013) *Biochemistry* 52, 1594−1602). Here we characterize the rate-limiting step for O_2 activation by FIH using a suite of mechanistic probes on the second order rate constant $k_{cat}/K_{M(O_2)}$. Steady-state kinetics showed that the rate constant for O_2 activation was slow ($k_{cat}/K^{app}_{M(O_2)}$ = 3500 M^{-1} s^{-1}) compared

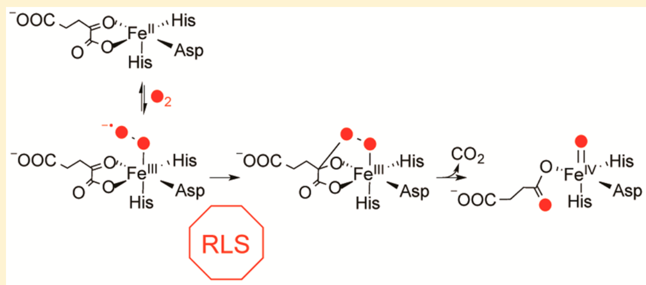

with other non-heme iron oxygenases, and solvent viscosity assays further excluded diffusional encounter with O_2 from being rate limiting on $k_{cat}/K_{M(O_2)}$. Competitive oxygen-18 kinetic isotope effect measurements ($^{18}k_{cat}/K_{M(O_2)}$ = 1.0114(5)) indicated that the transition state for O_2 activation resembled a cyclic peroxohemiketal, which precedes the formation of the ferryl intermediate observed in related enzymes. We interpret this data to indicate that FIH limits its overall activity at the point of the nucleophilic attack of Fe-bound O_2^- on the C-2 carbon of αKG. Overall, these results show that FIH follows the consensus mechanism for αKG oxygenases, suggesting that FIH may be an ideal enzyme to directly access steps involved in O_2 activation among the broad family of αKG oxygenases.

Mammalian cells respond to decreased cellular pO_2 levels through the enzyme-catalyzed reaction of O_2 with the hypoxia inducible factor-1α (HIF-1α or HIF).[1] HIF mediates the transcription of hundreds of genes in response to hypoxia[2] with the functions of the gene products ranging from glucose and iron metabolism to cell proliferation and angiogenesis.[3,4] Factor inhibiting HIF (FIH) is a non-heme Fe(II)/αKG oxygenase that turns-off the transcriptional activity of HIF[5,6] by hydroxylating the β-carbon of Asn[803] within the C-terminal activation domain (CTAD) of HIF (Scheme 1).[7−9] Because O_2 activation chemistry is central to hypoxia sensing by HIF, identifying the chemical steps involved in O_2 activation may point the way to methods for perturbing HIF-controlled gene expression.

FIH is proposed to follow the consensus mechanism for Fe(II)/αKG oxygenases (Scheme 1) for which the steps are supported to varying degrees by spectroscopic, computational, and kinetic studies.[10−15] VTVH MCD methodologies have been used to spectroscopically identify the release of the aquo ligand upon substrate binding to FIH[16] and other Fe(II)/αKG oxygenases including TauD and CAS.[17,18] O_2 is thought to bind as a ferric superoxide at the open coordination site and then attacks the C-2 carbonyl of αKG to ultimately form succinate and a ferryl intermediate. The molecular details following O_2 activation, including isolation of the ferryl intermediate and observation of HAT have been characterized in the Fe(II)/αKG oxygenases TauD[15,19−24] and P4H[25] and the related Fe(II)/αKG halogenases CytC3[26] and SyrB2.[27]

In contrast to the steps following ferryl formation, those steps of O_2 activation are poorly understood. Computational studies suggest that nucleophilic attack on the C-2 carbonyl of αKG is the rate-limiting step on $k_{cat}/K_{M(O_2)}$, with a cyclic peroxohemiketal proposed as the transition state.[28−30] Although this reaction sequence is supported by pre-steady-state kinetics and an oxygen-18 kinetic isotope effect (^{18}O KIE) study of TauD,[31] insight into O_2 activation is limited because HAT or product release is rate-limiting in TauD and other well-characterized αKG oxygenases.[20,32,33] Consequently, O_2 activation is too rapid to allow for the identification of any intermediates prior to the ferryl.

Recent studies showed that the rate-limiting step for FIH differed from that of other characterized αKG oxygenases.[16,34] Upon FIH binding to CTAD, there is partial retention of the aquo ligand[16] suggesting that aquo release may be less facile in FIH than in other enzymes. The inverse SKIE on k_{cat}[34] for FIH

Received: October 2, 2014
Revised: November 20, 2014
Published: November 25, 2014

dx.doi.org/10.1021/bi501246v | *Biochemistry* 2014, 53, 8077−8084

Scheme 1. Consensus Chemical Mechanism of αKG Oxygenases, Adapted for FIH

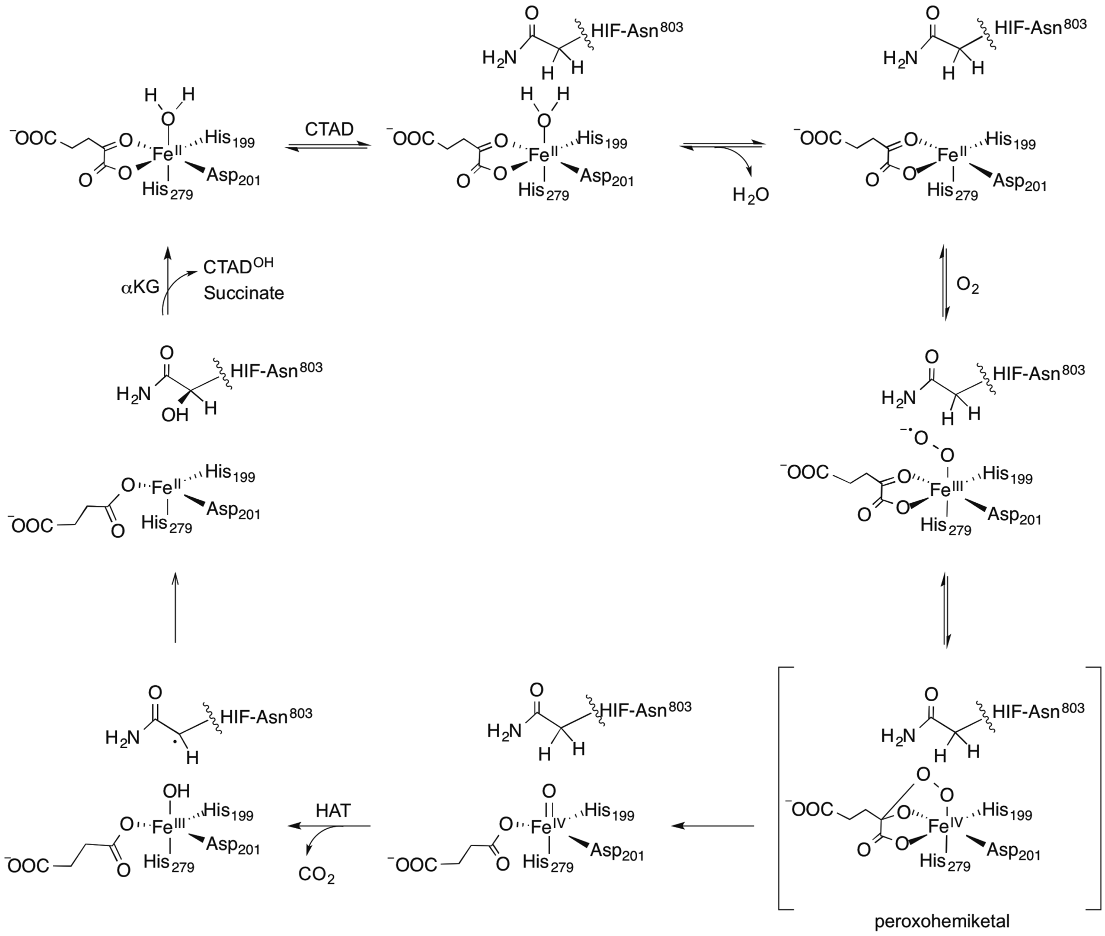

indicates that the aquo release reaches equilibrium prior to an irreversible step that is the overall rate-limiting step in FIH; in other words, the overall rate limiting step either precedes or coincides with the formation of the ferryl. This suggests that FIH either deviates from the consensus chemical mechanism or could provide a unique system to access other steps of mechanistic interest. In this work, we probe $k_{cat}/K_{M(O_2)}$, which focuses on the limited subset of steps that are involved in binding and reacting with O_2, to understand O_2 activation by FIH. Steady-state kinetics under conditions of varied solvent viscosity indicated that diffusional encounter of O_2 with FIH was not rate limiting on $k_{cat}/K_{M(O_2)}$. Furthermore, we determined the ^{18}O KIE on $k_{cat}/K_{M(O_2)}$ ($^{18}k_{cat}/K_{M(O_2)}$ = 1.0114(5)), identifying the rate-limiting step as formation of the peroxohemiketal. This showed that the chemical steps of O_2 activation on FIH followed the consensus mechanism, indicating that FIH only differs from other αKG oxygenases in that this O_2 activation step is the overall rate-limiting step during turnover.[34]

MATERIALS AND METHODS

Materials. All reagents were purchased from commercial sources and used as received unless noted. The sequences of the synthetic 19- and 39-mer CTAD peptides corresponded to the C-terminal activation domain (CTAD) of HIF-1$\alpha^{788-806}$ and HIF-1$\alpha^{788-826}$, respectively, with a Cys^{800} → Ala point mutation. Peptides were purchased from EZBiolab (Carmel, Indiana, USA) with free N- and C-termini. The CTAD$^{788-806}$ peptide (purity >95%) was used without further purification; however CTAD$^{788-826}$ was purchased as a desalted peptide and purified to >95% purity using RP-HPLC as previously described.[34]

Protein Expression and Purification. FIH was overexpressed in *Escherichia coli* and purified as previously reported.[34,35] Thrombin cleavage of the His$_6$ tag led to three additional residues preceding the native sequence of FIH on the N-terminus (NH$_2$-Gly-Ser-His-). The purity of the protein (>95%) was assessed through SDS-PAGE.

Steady-State Kinetic Assays with Varying O_2. All assays were performed in an AtmosBag (Sigma-Aldrich) with the O_2 concentration of the reaction buffers equilibrated to the O_2 partial pressue within the bag. The atmosphere of the bag was equilibrated for 30 min with a controlled mixture of N_2 and O_2. HEPES, pH 7.00 (50 mM) was gently stirred for 5 min in a 37.0 °C water bath to equilibrate the reaction buffer with the atmosphere, and then the O_2 concentration was measured using a Clarke electrode.

Steady-state assays in which O_2 was the varied substrate (0.020−1 mM) utilized a fixed CTAD$^{788-826}$ concentration of either 80 μM ($\sim K_{M(CTAD)}$) or 150 μM ($\sim 2K_{M(CTAD)}$) and saturating concentrations of FeSO$_4$ (25 μM), αKG (100 μM), and ascorbate (2 mM), prepared in 50 mM HEPES, pH 7.00. Upon addition of all reagents except FIH, the reaction mixture (45 μL) was incubated at 37.0 °C for an additional 2 min. The enzyme stock was equilibrated to the atmosphere by gently

dx.doi.org/10.1021/bi501246v | Biochemistry 2014, 53, 8077−8084

pipetting the solution down the side of the microcentrifuge tube, before injecting an aliquot (5 μL) to initiate the assays. Reaction aliquots were removed throughout a 3 min time course, quenched in 75% acetonitrile/0.2% TFA (20 μL) saturated with 3,5-dimethoxy-4-hydroxycinnamic acid and analyzed for the initial rate of formation of CTAD^{OH} using a Bruker microFlex MALDI-TOF-MS. Initial rates were determined as previously described[34] and fit to the Michaelis−Menten equation resulting in the apparent kinetic parameters k_{cat}, $k_{cat}/K_{M(O_2)}$, and $K_{M(O_2)}$.

Solvent Viscosity Effect. Assays to test for rate-limiting diffusional encounter of O_2 utilized a fixed CTAD$^{788-826}$ concentration of 80 μM ($\sim K_{M(CTAD)}$) and saturating concentrations of $FeSO_4$ (25 μM), αKG (100 μM), and ascorbate (2 mM), with the exception of the addition of sucrose (25% w/w) to the 50 mM HEPES, pH 7.00, to give a relative visocity of η/η_0 = 2.4.[36] Reactions were performed as described above to determine initial rates with O_2 as the varied substrate, which were then fit to the Michaelis−Menten equation.

Steady-State Kinetic Assays with CTAD$^{788-806}$. Assays in which CTAD$^{788-806}$ was varied (0.10−4.6 mM) were performed at 37.0 °C in 50 mM HEPES, pH 7.00, and contained ascorbate (2 mM), αKG (1 mM), $FeSO_4$ (50 μM), and an ambient O_2 concentration (217 μM). Assays in which αKG was varied (0.005−1 mM) were also performed at 37.0 °C in 50 mM HEPES, pH 7.00, and contained ascorbic acid (2 mM), $FeSO_4$ (50 μM), and CTAD$^{788-806}$ (750 μM), with an ambient O_2 concentration (217 μM). Reagents were mixed and incubated at 37.0 °C for 2 min before initiating turnover with enzyme (5−20 μM). At predetermined time points, aliquots were quenched in 75% acetonitrile/0.2% TFA (20 μL) saturated with α-cyano-4-hydroxycinnamic acid. Initial rates were detemined as described above and fit to the Michaelis−Menten equation resulting in the apparent kinetic parameters k_{cat}, k_{cat}/K_M, and K_M.

^{18}O KIE Sample Preparation and Analysis. Assays used to determine the ^{18}O KIE contained αKG (1.0 mM), CTAD$^{788-806}$ (250 μM), $FeSO_4$ (50 μM), and O_2 (280 μM) in 50 mM HEPES, pH 7.00. Buffer was equilibrated to ambient O_2 concentration (280 μM) by gently stirring for 2 days at 21 °C. All reagents were prepared freshly using the equilibrated buffer and gently mixed to make a common reaction mixture. This reaction mixture was injected into a 10 mL crimp vial sealed with a butyl rubber stopper (Geo-Microbial Technologies, Inc.; Ochelata, OK), ensuring all air was removed. After a 3 min incubation of the vial at 37.0 °C, each reaction was initiated with an injection (20 μL) of a high concentration FIH stock that had been equilibrated to room temperature (21 °C). Reactions were quenched using 6 M HCl, 3.5 M $ZnCl_2$ (40 μL) after an extended reaction time such that the fractional conversion based on O_2 was as high as 35%. An aliquot (5 μL) was removed to determine the reaction progress by measuring CTAD^{OH} formation using a Bruker MALDI-TOF-MS. The quantity of CTAD^{OH} produced was used to determine the fractional conversion of O_2 for each quenched reaction. The sealed crimp vials containing the quenched reactions were stored inverted and submerged in water until analysis by isotope-ratio mass spectrometry (IRMS).

The ^{18}O KIE samples were carefully transferred into pre-evacuated 25 mL glass vessels fitted with a glass high vacuum stopcock (Chemglass). The filling procedure is described in detail by Emerson et al.[37] but briefly consisted of flushing the neck of the bottle with a gentle stream of CO_2 to displace air followed by introduction of sample water from a small diameter tubing (~3 mm) to the bottleneck. Upon opening the stopcock slowly, sample water is drawn into the evacuated bottle until the bottle is approximately half full. The headspace gases and water are then equilibrated by gently shaking in a 25 °C water bath overnight. Before IRMS analysis, the sample water was removed using aspiration, leaving ~0.5 mL of sample in the bottle. Headspace gases in the bottle were then analyzed for the δ^{18}O of O_2 using a gas chromatograph interfaced to an Elementar Isoprime IRMS.[38] All δ^{18}O isotopic values were reported using standard delta notation relative to the Vienna standard mean ocean water (VSMOW).[39] Equation 1 was used to convert the δ^{18}O to an R value ($^{18}O/^{16}O$ isotopic ratio), where R_{std} is the standard isotopic value for O_2 in air (0.0020531)[40] and R_f is the $^{18}O/^{16}O$ isotopic ratio at O_2 fractional conversion f.

$$R_f = \left(\frac{\delta^{18}O}{1000} + 1\right)R_{std} \tag{1}$$

To determine the $^{18}O/^{16}O$ isotopic ratio at t = 0 (R_0), a sample was prepared from the common reaction stock containing αKG (1.0 mM), CTAD$^{788-806}$ (250 μM), $FeSO_4$ (50 μM), and O_2 (280 μM) in 50 mM HEPES, pH 7.00, and injected into a sealed crimp vial. After incubation for 3 min at 37.0 °C, an aliquot of 50 mM HEPES, pH 7.00 (20 μL), was injected into the vial immediately followed by an injection (40 μL) of 6 M HCl, 3.5 M $ZnCl_2$ to quench the reaction.

The ^{18}O KIE was determined by fitting R_f/R_0 vs f to eq 2, where f is the fractional conversion of O_2 in the reaction aliquot, R_f *is* the $^{18}O/^{16}O$ isotope ratio of the aliquot, and R_0 is the $^{18}O/^{16}O$ isotope ratio of the blank.

$$\frac{R_f}{R_0} = (1 - f)^{(1/^{18}\text{O-KIE}) - 1} \tag{2}$$

RESULTS AND DISCUSSION

The O_2 activation mechanisms of Fe(II)/αKG oxygenases are of enormous interest due to the biomedical significance of these enzymes.[12,41,42] FIH hydroxylates the HIF transcription factor for hypoxia sensing, and other members are involved in processes such as DNA and RNA repair and histone demethylation,[12,43,44] placing some of these enzymes into biological roles that are more concerned with regulation than with bulk turnover of metabolites. A crucial mechanistic feature of these enzymes is O_2 activation to form an active oxidant, identified in several enzymes as a ferryl species.[19,25,26] Despite the importance of the chemical steps leading up to formation of the ferryl, these steps remain largely uncharacterized. Because the overall rate-limiting step for FIH either precedes or coincides with ferryl formation,[34] FIH could be an excellent enzyme to interrogate steps involved in O_2 activation that are common to other αKG oxygenases, provided that FIH follows the consensus mechanism.

Steady-State Kinetics with Varying O_2. To characterize the steps limiting the rate of O_2 activation by FIH, steady-state kinetic assays with O_2 as the varied substrate were performed using a fixed CTAD$^{788-826}$ concentration. Because our assays used subsaturating CTAD concentration due to reagent expenses, these steady-state assays used two different

CTAD[788−826] concentrations to measure the second order rate constant, $k_{cat}/K_{M(O_2)}$.

The initial rate data using 80 μM CTAD[788−826] was fit to the Michaelis−Menten equation with kinetic parameters of k_{cat}^{app} = 33 ± 3 min^{-1} and $k_{cat}/K_{M(O_2)}^{app}$ = 0.17 ± 0.03 μM^{-1} min^{-1} (Figure 1, Table 1). The steady-state assays with varying O_2 using an increased CTAD concentration (150 μM) resulted in $k_{cat}/K_{M(O_2)}^{app}$ = 0.21 ± 0.04, which is statistically equivalent to the $k_{cat}/K_{M(O_2)}^{app}$ at 80 μM CTAD[788−826]. These results indicated that $k_{cat}/K_{M(O_2)}$ was independent of CTAD concentration as expected for the sequential consensus mechanism (Scheme 1). The high value for the Michaelis constant ($K_{M(O_2)}^{app}$ > 200 μM) was in agreement with previous reported values (90−237 μM) obtained using oxygen consumption assays and $^{14}CO_2$ capture assays[45,46] and is thought to be essential for a proportionate sensory response by FIH to increasing pO_2.

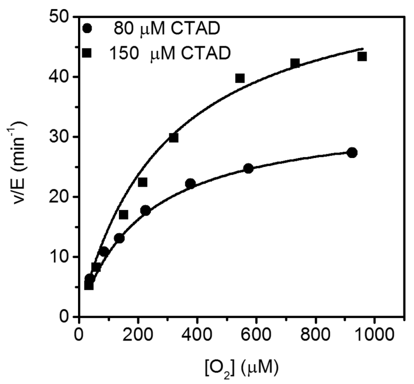

Figure 1. Steady-state kinetics with varying O_2. Reactions contained FIH (0.25−0.5 μM), ascorbate (2 mM), αKG (100 μM), $FeSO_4$ (25 μM), and CTAD[788−826] (80 μM,●, or 150 μM, ■) in 50 mM HEPES, pH 7.00, 37.0 °C.

Table 1. Apparent Kinetic Parameters for FIH with Varied O_2 Concentration[a]

[CTAD[788−826]] (μM)	k_{cat}^{app} (min^{-1})	$k_{cat}/K_{M(O_2)}^{app}$ (μM^{-1} min^{-1})	$K_{M(O_2)}^{app}$ (μM)
80	33 ± 3.0	0.17 ± 0.03	200 ± 40
150	54 ± 4.0	0.21 ± 0.04	270 ± 50

[a]Reactions contained ascorbate (2 mM), αKG (100 μM), $FeSO_4$ (25 μM), and CTAD[788−826] in 50 mM HEPES, pH 7.00, 37.0 °C.

When converted into standard units, $k_{cat}/K_{M(O_2)}^{app}$ = 3.5 × 10^3 M^{-1} s^{-1}, it was clear that the rate constant for O_2 activation in FIH was significantly slower than those for non-heme iron oxygenases that are not involved in O_2 concentration sensing, such as TauD (1.5 × 10^5 M^{-1} s^{-1}),[33,47] tyrosine hydroxylase (6.0 × 10^4 M^{-1} s^{-1}),[48] and lipoxygenase (∼5.0 × 10^5 M^{-1} s^{-1}).[49,50] In contrast, the slow rate constant for O_2 activation and the high Michaelis constant for O_2 found for FIH are found in those non-heme iron oxygenases implicated in O_2 sensing, such as PHD2[51] and Jumonji C domain-containing histone demethylases.[52] The small magnitude of $k_{cat}/K_{M(O_2)}$ for FIH is intriguing, raising the potential for FIH and these putative O_2 sensors to use an unusual strategy for O_2 activation. Although it is likely that a slow chemical step limits $k_{cat}/K_{M(O_2)}$ and O_2 activation, it was necessary to test diffusional encounter as a possibility for the rate-limiting step.

Solvent Viscosity Effect. To test for diffusional encounter with O_2 as a partially rate-limiting step on $k_{cat}/K_{M(O_2)}$, we performed steady-state assays under varied solvent viscosity. Although $k_{cat}/K_{M(O_2)}$ is orders of magnitude slower than expected for a diffusional process (ca. 1 × 10^9 M^{-1} s^{-1}), we could not dismiss the possibility that there was an unfavorable pre-equilibrium leading to a very small fraction of FIH being competent for reaction upon collision. For diffusion controlled processes, $k_{cat}/K_{M(O_2)}$ would decrease in the presence of added viscosogen due to a lower diffusion rate as observed for other enzymes such as superoxide dismutase[53,54] and carbonic anhydrase.[55,56]

Our assays were performed as described above in the presence and absence of the viscosgen sucrose, giving a final relative viscosity (η/η_o) of 1.0 and 2.4, respectively (Figure 2).

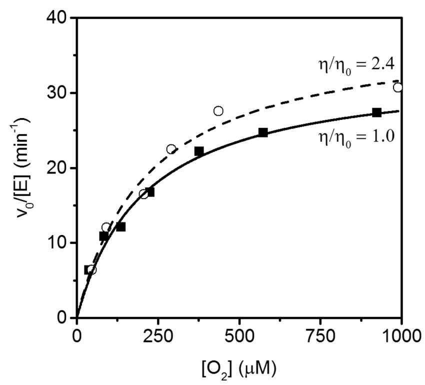

Figure 2. Steady-state kinetics with varying O_2: 0% sucrose (solid line, η/η_o = 1) and 25% sucrose (dashed line, η/η_o = 2.4). Assays contained ascorbate (2 mM), αKG (100 μM), $FeSO_4$ (25 μM), CTAD[788−826] (80 μM), and sucrose (0% or 25%) in 50 mM HEPES, pH 7.00, 37.0 °C.

At increased solvent viscosity, the resulting kinetic parameter $k_{cat}/K_{M(O_2)}^{app}$ = 0.18 ± 0.04 μM^{-1} min^{-1} was indistinguishable from the kinetic parameter collected in the absence of viscosogen (Table 2). The resulting insignificant solvent viscosity effect on $k_{cat}/K_{M(O_2)}$ indicated that diffusional encounter with O_2 did not limit the rate constant for O_2 activation in FIH.

Table 2. Solvent Viscosity Effect on $k_{cat}/K_{M(O_2)}$[a]

η/η_o	k_{cat}^{app} (min^{-1})	$k_{cat}/K_{M(O_2)}^{app}$ (μM^{-1} min^{-1})	$K_{M(O_2)}^{app}$ (μM)
1.0	33 ± 3.0	0.17 ± 0.03	200 ± 40
2.4	39 ± 3.0	0.18 ± 0.04	220 ± 43

[a]Assays contained ascorbate (2 mM), αKG (100 μM), $FeSO_4$ (25 μM), CTAD[788−826] (80 μM), and sucrose (0% or 25% w/w) in 50 mM HEPES, pH 7.00, 37.0 °C.

Diffusion limited rate constants may be found with enzymes that have achieved catalytic perfection, reflecting a physiological role that requires bulk turnover of a large quantity of substrate. For example, diffusion limited rate constants fit well for SOD's cellular function to scavenge superoxide to minimize oxidative damage.[57] As an O_2 sensor, one would imagine that FIH turnover could be limited by collisional encounter. However, the absence of a viscosity effect on $k_{cat}/K_{M(O_2)}$ and k_{cat} showed that FIH was not diffusionally limited under varied O_2 concentration. This implicates a chemical step as rate-limiting under conditions of low O_2 concentration, consistent with prior results indicating that k_{cat} was limited by a step that followed aquo release but preceded the HAT.[34]

Competitive ^{18}O Kinetic Isotope Effect. Because $k_{cat}/K_{M(O_2)}$ encompasses all steps between diffusional collision of FIH with O_2 through the subsequent irreversible step, the ^{18}O heavy atom isotope effect on this rate constant is an ideal reporter of the rate-limiting step. We employed competitive $^{18}O/^{16}O$ KIE measurements using O_2 at natural isotopic abundance to identify the rate limiting step on $k_{cat}/K_{M(O_2)}$ in FIH. The $^{18}O/^{16}O$ isotopic abundance of residual O_2 was measured by IRMS from quenched reactions of FIH, which were fit to eq 2 resulting in a $^{18}k_{cat}/K_{M(O_2)}$ = 1.0114(5) (Figure 3). Because the typical range of values for $^{18}k_{cat}/K_{M(O_2)}$ is 1.00–1.03, this places O_2 activation by FIH in a clear context when considered next to the mechanisms followed by other non-heme Fe enzymes.[31]

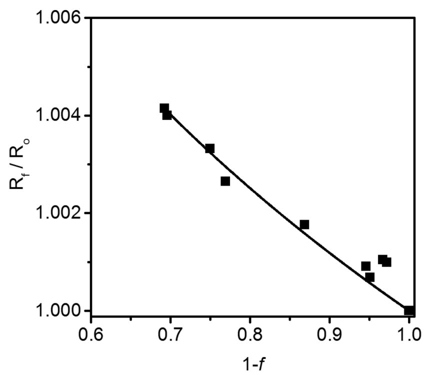

Figure 3. ^{18}O fractionation (R_f/R_0) versus the fractional conversion of O_2 in quenched reactions of FIH. Each reaction contained αKG (1.0 mM), CTAD$^{788-806}$ (250 μM), $FeSO_4$ (50 μM), and O_2 (280 μM) in 50 mM HEPES, pH 7.00, 37.0 °C. Data are fit to eq 2; $^{18}k_{cat}/K_{M(O_2)}$ = 1.0114(5).

$^{18}k_{cat}/K_{M(O_2)}$ reflects the changes in O–O bonding between molecular O_2 and the transition state of the kinetically irreversible step on $k_{cat}/K_{M(O_2)}$.[58,59] Because the ^{18}O equilibrium isotope effect (^{18}O EIE) provides an upper limit for the ^{18}O KIE,[60] previously calculated ^{18}O EIEs for the equilibrium $Fe^{2+} + O_2 \Leftrightarrow X$ provide an excellent yardstick for the transition state structure based upon the value of $^{18}k_{cat}/K_{M(O_2)}$ (Chart 1).[31] For example, the calculated ^{18}O EIE for X = $Fe^{3+}(O_2^-)$ is small (^{18}O EIE = 1.0080),[31] meaning that rate-limiting formation of this intermediate would lead to a correspondingly small value for $^{18}k_{cat}/K_{M(O_2)}$. A larger ^{18}O EIE is calculated for X = ferric peroxo-carbonate (^{18}O EIE =1.0129),[31] a structure resembling the putative peroxohemiketal, which is in good agreement with the observed $^{18}k_{cat}/K_{M(O_2)}$ for FIH, suggesting that the rate-limiting step for FIH proceeds through a transition state that resembles this structure. In contrast, the observed $^{18}k_{cat}/K_{M(O_2)}$ is inconsistent with the ^{18}O EIE calculated for X = ferryl (^{18}O EIE = 1.0287),[31] indicating that the ferryl intermediate is formed after the rate-limiting step on $k_{cat}/K_{M(O_2)}$ in FIH.

Chart 1. Proposed Transition State Structures from ^{18}O EIE[a]

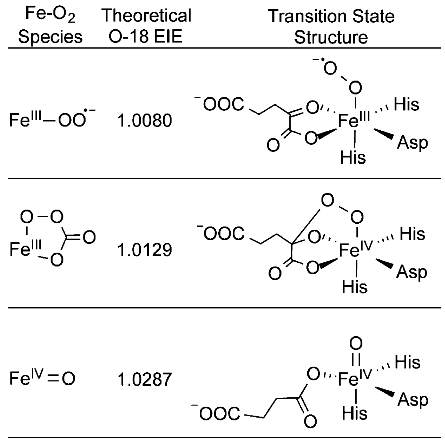

[a] ^{18}O EIE values were calculated in ref 31.

$^{18}k_{cat}/K_{M(O_2)}$ has been utilized to study the O_2 activation pathways of other non-heme iron enzymes including soluble methane monooxygenase,[61] ACCO,[62] TauD,[31] HppE,[31] and tyrosine hydroxylase.[63] In each case, the magnitude of $^{18}k_{cat}/K_{M(O_2)}$ provided important insight into the chemical strategy followed for O_2 activation. For those enzymes in which O_2 binds at Fe^{2+}, the initial step is the reversible formation of a $Fe^{3+}(O_2^-)$ adduct, which subsequently requires electrons from cofactor or (co)substrate to activate the O–O bond for chemistry. In the case of TauD, this activation takes the form of a nucleophilic attack of the $Fe^{3+}(O_2^-)$ on the C-2 keto position of αKG.[31]

The $^{18}k_{cat}/K_{M(O_2)}$ for FIH (1.0114(5)) is very similar to that observed for TauD ($^{18}k_{cat}/K_{M(O_2)}$ = 1.0102),[31] indicating a common transition state structure for αKG decarboxylation in these two enzymes. The larger value for the $^{18}k_{cat}/K_{M(O_2)}$ for FIH than for TauD is likely due to the slower turnover rate of FIH. The observed $^{18}k_{cat}/K_{M(O_2)}$ will approach the ^{18}O EIE when the forward commitment, which is the ratio of the forward and reverse rate constants for disappearance of the species immediately preceding the rate-limiting step, is small as might be expected for the slower chemistry in FIH.

The chemical strategy for O_2 activation in αKG oxygenases was predicted by DFT calculations to proceed through the nucleophilic attack on the αKG cofactor[28,29] and is supported by the ^{18}O KIE results. The self-consistent field (SCF) calculations predicted that decomposition of the initially formed cyclic peroxohemiketal intermediate was barrierless[29] leading to decarboxylation with the formation of a Fe^{2+}(peroxysuccinate) intermediate prior to formation of the ferryl(succinate). Because the decarboxylation is irreversible, $k_{cat}/K_{M(O_2)}$ only reports on steps between the collision with O_2 and this decarboxylation step (Scheme 2).

Studies to date that address O_2 activation chemistry in αKG oxygenases have relied on steady-state mechanistic probes and

Scheme 2. O_2 Activation in αKG Oxygenases

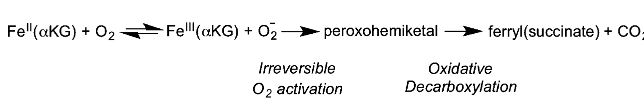

dx.doi.org/10.1021/bi501246v | Biochemistry 2014, 53, 8077–8084

point mutagenesis[22,45,64−67] and suggest that hydrogen bonding contacts to the αKG play an important role in facilitating decarboxylation. Further insight into oxidative decarboxylation has been hampered by the identity of the rate limiting steps in TauD and other αKG oxygenases. In the cases of TauD,[20] P4H,[25] CytC3,[32] and by analogy DAOCS[68] and the histone demethylase KDM4E,[69] HAT by the ferryl or product release are partially rate-limiting on turnover at elevated O_2 concentration, preventing the accumulation of any species involved in O_2 activation during the pre-steady-state. A crucial difference between these other enzymes and FIH is that several lines of evidence indicate that decarboxylation is rate limiting in FIH, suggesting that FIH may allow direct access to steps involved in O_2 activation.

■ CONCLUSIONS

We have used multiple kinetic probes to characterize O_2 activation by FIH. Unlike other previously characterized Fe(II)/αKG enzymes, turnover in FIH is fully limited by the rate of O_2 activation. This kinetic feature is consistent with the function of FIH as an O_2 sensor; strong oxidants such as the ferryl would be short-lived, ensuring tight coupling between O_2 activation and CTAD hydroxylation. It may be possible that other biomedically important Fe(II)/αKG enzymes such as the JmjC and JmjD domain-containing hydroxylases and PHD2 employ a similar mechanistic strategy to regulate their function. If so, rate-limited O_2 activation may be a more common mechanistic feature among Fe(II)/αKG oxygenases than is currently appreciated.

■ ASSOCIATED CONTENT

Supporting Information

Control experiments involving steady-state kinetics with the CTAD[788−806] peptide, as well as steady-state kinetics in the presence and absence of ascorbate. The material is available free of charge via the Internet at http://pubs.acs.org.

■ AUTHOR INFORMATION

Corresponding Author

*E-mail: mknapp@chem.umass.edu. Voice: (413) 545-4001. Fax: (413) 545-4490.

Funding

This research was supported by the U.S. National Institutes of Health (Grant 1R01-GM077413 to M.J.K.) and the National Science Foundation (Grant EAR-1053432) to N.E.O. J.A.H. was supported in part by the NIH Chemistry-Biology Interface Predoctoral Training Grant T32-GM008515.

Notes

The authors declare no competing financial interest.

■ ABBREVIATIONS

ACCO, 1-aminocyclopropane-1-carboxylic acid oxidase; αKG, α-ketoglutarate; CAS, clavaminate synthase; CTAD, C-terminal transactivation domain; DFT, density functional theory; EIE, equilibrium isotope effect; FIH, factor-inhibiting HIF; HAT, hydrogen atom transfer; HEPES, 4-(2-hydroxyethyl)-1-piperazineethanesulfonic acid; HIF, hypoxia inducible factor-1α; HppE, (*S*)-2-hydroxypropyl-1-phosphonate epoxidase; IRMS, isotope ratio mass spectrometry; KIE, kinetic isotope effect; MALDI-TOF-MS, matrix assisted laser desorption ionization-time-of-flight-mass spectrometry; MCD, magnetic circular dichroism; P4H, prolyl-4-hydroxylase; PHD2, prolyl hydroxylase domain 2; SKIE, solvent kinetic isotope effect; SCF, self-consistent field; SOD, superoxide dismutase; TauD, taurine dioxygenase; TFA, trifluoroacetic acid; VTVH, variable temperature variable field

■ REFERENCES

(1) Taabazuing, C. Y., Hangasky, J. A., and Knapp, M. J. (2014) Oxygen sensing strategies in mammals and bacteria. *J. Inorg. Biochem. 133*, 63−72.

(2) Mole, D. R., Blancher, C., Copley, R. R., Pollard, P. J., Gleadle, J. M., Ragoussis, J., and Ratcliffe, P. J. (2009) Genome-wide Association of Hypoxia-inducible Factor (HIF)-1a and HIF-2a DNA Binding with Expression Profiling of Hypoxia-inducible Transcripts. *J. Biol. Chem. 284*, 16767−16775.

(3) Ke, Q., and Costa, M. (2006) Hypoxia-Inducible Factor-1 (HIF-1). *Mol. Pharmacol. 70*, 1469−1480.

(4) Semenza, G. L. (2003) Targeting HIF-1 for cancer therapy. *Nat. Rev. Cancer 3*, 721−732.

(5) Metzen, E., and Ratcliffe, P. J. (2004) HIF hydroxylation and cellular oxygen sensing. *Biol. Chem. 385*, 223−230.

(6) Schofield, C. J., and Ratchliffe, P. J. (2004) Oxygen sensing by HIF-hydroxylases. *Nat. Rev. Mol. Cell Biol. 5*, 343−354.

(7) Lando, D., Peet, D. J., Gorman, J. J., Whelan, D. A., Whitelaw, M. L., and Bruick, R. K. (2002) FIH-1 is an asparaginyl hydroxylase enzyme that regulates the transcriptional activity of hypoxia-inducible factor. *Genes Dev. 16*, 1466−1471.

(8) McNeill, L. A., Hewitson, K. S., Claridge, T. D., Seibel, J. F., Horsfall, L. E., and Schofield, C. J. (2002) Hypoxia-inducible factor asparaginyl hydroxylase (FIH-1) catalyses hydroxylation at the beta-carbon of asparagine-803. *Biochem. J. 367*, 571−575.

(9) Lando, D., Peet, D. J., Whelan, D. A., Gorman, J. J., and Whitelaw, M. L. (2002) Asparagine hydroxylation of the HIF transactivation domain a hypoxic switch. *Science 295*, 858−861.

(10) Solomon, E. I., Light, K. M., Liu, L. V., Srnec, M., and Wong, S. D. (2013) Geometric and Electronic Structure Contributions to Function in Non-heme Iron Enzymes. *Acc. Chem. Res. 46*, 2725−2739.

(11) Blomberg, M. R. A., Borowski, T., Himo, F., Liao, R. Z., and Siegbahn, P. E. M. (2014) Quantum Chemical Studies of Mechanisms for Metalloenzymes. *Chem. Rev. 114*, 3601−3658.

(12) Hausinger, R. P. (2004) Fe(II)/alpha-Ketoglutarate-dependent hydroxylases and related enzymes. *Crit. Rev. Biochem. Mol. Biol. 39*, 21−68.

(13) Aik, W., McDonough, M. A., Thalhammer, A., Chowdhury, R., and Schofield, C. J. (2012) Role of the jelly-roll fold in substrate binding by 2-oxoglutarate oxygenases. *Curr. Opin. Struct. Biol. 22*, 691−700.

(14) Bollinger, J. M., Price, J. C., Hoffart, L. M., Barr, E. W., and Krebs, C. (2005) Mechanism of Taurine: α-Ketoglutarate Dioxygenase (TauD) from *Escherichia coli*. *Eur. J. Inorg. Chem. 2005*, 4245−4254.

(15) Grzyska, P. K., Appelman, E. H., Hausinger, R. P., and Proshlyakov, D. A. (2010) Insight into the mechanism of an iron dioxygenase by resolution of steps following the FeIV=HO species. *Proc. Natl. Acad. Sci. U. S. A. 107*, 3982−3987.

(16) Light, K. M., Hangasky, J. A., Knapp, M. J., and Solomon, E. I. (2013) Spectroscopic Studies of the Mononuclear Non-Heme Fe-II Enzyme FIH: Second-Sphere Contributions to Reactivity. *J. Am. Chem. Soc. 135*, 9665−9674.

(17) Neidig, M. L., Brown, C. D., Light, K. M., Fujimori, D. G., Nolan, E. M., Price, J. C., Barr, E. W., Bollinger, J. M., Krebs, C., Walsh, C. T., and Solomon, E. I. (2007) CD and MCD of CytC3 and taurine dioxygenase: role of the facial triad in alpha-KG-dependent oxygenases. *J. Am. Chem. Soc. 129*, 14224−14231.

(18) Zhou, J., Kelly, W. L., Bachmann, B. O., Gunsior, M., Townsend, C. A., and Solomon, E. I. (2001) Spectroscopic studies of substrate interactions with clavaminate synthase 2, a multifunctional alpha-KG-dependent non-heme iron enzyme: Correlation with mechanisms and reactivities. *J. Am. Chem. Soc. 123*, 7388−7398.

(19) Price, J. C., Barr, E. W., Tirupati, B., Bollinger, J. M., and Krebs, C. (2003) The First Direct Characterization of a High-Valent Iron Intermediate in the Reaction of an a-Ketoglutarate-Dependent Dioxygenase: A High-Spin Fe(IV) Complex in Taurine/a-Ketoglutarate Dioxygenase (TauD) from Escherichia coli. *Biochemistry 42*, 7497−7508.

(20) Price, J. C., Barr, E. W., Glass, T. E., Krebs, C., and Bollinger, J. M. (2003) Evidence for Hydrogen Abstraction from C1 of Taurine by the High-Spin Fe(IV) Intermediate Detected during Oxygen Activation by Taurine:a-Ketoglutarate Dioxygenase (TauD). *J. Am. Chem. Soc. 125*, 13008−13009.

(21) Riggs-Gelasco, P. J., Price, J. C., Guyer, R. B., Brehm, J. H., Barr, E. W., Bollinger, J. M., and Krebs, C. (2004) EXAFS spectroscopic evidence for an Fe = O unit in the Fe(IV) intermediate observed during oxygen activation by taurine:alpha-ketoglutarate dioxygenase. *J. Am. Chem. Soc. 126*, 8108−8109.

(22) Grzyska, P. K., Ryle, M. J., Monterosso, G. R., Liu, J., Ballou, D. P., and Hausinger, R. P. (2005) Steady-State and Transient Kinetic Analyses of Taurine/alpha-Ketoglutarate Dioxygenase: Effects of Oxygen Concentration, Alternative Sulfonates, and Active-Site Variants on the FeIV-oxo Intermediate. *Biochemistry 44*, 3845−3855.

(23) Proshlyakov, D. A., Henshaw, T. F., Monterosso, G. R., Ryle, M. J., and Hausinger, R. P. (2004) Direct Detection of Oxygen Intermediates in the Non-Heme Fe Enzyme Taurine/alpha-Ketoglutarate Dioxygenase. *J. Am. Chem. Soc. 126*, 1022−1023.

(24) Ryle, M. J., Padmakumar, R., and Hausinger, R. P. (1999) Stopped-Flow Kinetic Analysis of *Escherichia coli* Taurine/alpha-Ketoglutarate Dioxygenase: Interactions with alpha-Ketoglutarate, Taurine, and Oxygen. *Biochemistry 38*, 15278−15286.

(25) Hoffart, L. M., Barr, E. W., Guyer, R. B., Bollinger, J. M., and Krebs, C. (2006) Direct spectroscopic detection of a C-H-cleaving high-spin Fe(IV) complex in a prolyl-4-hydroxylase. *Proc. Natl. Acad. Sci. U. S. A. 103*, 14738−14743.

(26) Galonic Fujimori, D., Barr, E. W., Matthews, M. L., Koch, G. M., Yonce, J. R., Walsh, C. T., Bollinger, J. M., Jr., Krebs, C., and Riggs-Gelasco, P. J. (2007) Spectroscopic evidence for a high-spin Br-Fe(IV)-Oxo intermediate in the alpha-ketoglutarate-dependent halogenase CytC3 from Streptomyces. *J. Am. Chem. Soc. 129*, 13408−13409.

(27) Wong, S. D., Srnec, M., Matthews, M. L., Liu, L. V., Kwak, Y., Park, K., Bell, C. B., III, Alp, E. E., Zhao, J., Yoda, Y., Kitao, S., Seto, M., Krebs, C., Bollinger, J. M., Jr., and Solomon, E. I. (2013) Elucidation of the Fe(IV)═O intermediate in the catalytic cycle of the halogenase SyrB2. *Nature 499*, 320−323.

(28) Borowski, T., Bassan, A., and Siegbahn, P. E. M. (2004) Mechanism of dioxygen activation in 2-oxoglutarate-dependent enzymes: A hybrid DFT study. *Chem.—Eur. J. 10*, 1031−1041.

(29) Ye, S., Riplinger, C., Hansen, A., Krebs, C., Bollinger, J. M., and Neese, F. (2012) Electronic Structure Analysis of the Oxygen-Activation Mechanism by FeII- and α-Ketoglutarate (αKG)-Dependent Dioxygenases. *Chem.—Eur. J. 18*, 6555−6567.

(30) Topol, I. A., Nemukhin, A. V., Salnikow, K., Cachau, R. E., Abashkin, Y. G., Kasprzak, K. S., and Burt, S. K. (2006) Quantum chemical modeling of reaction mechanism for 2-oxoglutarate dependent enzymes: effect of substitution of iron by nickel and cobalt. *J. Phys. Chem. A 110*, 4223−4428.

(31) Mirica, L. M., McCusker, K. P., Munos, J. W., Liu, H., and Klinman, J. P. (2008) 18O kinetic isotope effects in non-heme iron enzymes: Probing the nature of Fe/O_2 intermediates. *J. Am. Chem. Soc. 130*, 8122−8123.

(32) Galonic, D. P., Barr, E. W., Walsh, C. T., Bollinger, J. M., Jr., and Krebs, C. (2007) Two interconverting Fe((IV)) intermediates in aliphatic chlorination by the halogenase CytC3. *Nat. Chem. Biol. 3*, 113−116.

(33) Price, J. C., Barr, E. W., Hoffart, L. M., Krebs, C., and Bollinger, J. M. (2005) Kinetic dissection of the catalytic mechanism of taurine:alpha-ketoglutarate dioxygenase (TauD) from *Escherichia coli*. *Biochemistry 44*, 8138−8147.

(34) Hangasky, J. A., Saban, E., and Knapp, M. J. (2013) Inverse Solvent Isotope Effects Arising from Substrate Triggering in the Factor Inhibiting Hypoxia Inducible Factor. *Biochemistry 52*, 1594−1602.

(35) Chen, Y. H., Comeaux, L. M., Herbst, R. W., Saban, E., Kennedy, D. C., Maroney, M. J., and Knapp, M. J. (2008) Coordination changes and auto-hydroxylation of FIH-1: Uncoupled O-2-activation in a human hypoxia sensor. *J. Inorg. Biochem. 102*, 2120−2129.

(36) (1981) *CRC Handbook of Chemistry and Physics*, 61st ed., CRC Press, Boca Raton, FL.

(37) Emerson, S., Quay, P., Stump, C., Wilbur, D., and Knox, M. (1991) Oxygen Argon Nitrogen and Radon-222 in Surface Waters of the Subarctic Ocean Net Biological Oxygen Production. *Global Biogeochem. Cycles 5*, 49−70.

(38) Roberts, B. J., Russ, M. E., and Ostrom, N. E. (2000) Rapid and Precise Determination of the δ18O of Dissolved and Gaseous Dioxygen via Gas Chromatography−Isotope Ratio Mass Spectrometry. *Environ. Sci. Technol. 34*, 2337−2341.

(39) Dansgaard, W. (1964) Stable Isotopes in Precipitation. *Tellus 16*, 436−468.

(40) Barkan, E., and Luz, B. (2005) High precision measurements of O-17/O-16 and O-18/O-16 ratios in H2O. *Rapid Commun. Mass Spectrom. 19*, 3737−3742.

(41) Nagel, S., Talbot, N. P., Mecinovic, J., Smith, T. G., Buchan, A. M., and Schofield, C. J. (2010) Therapeutic manipulation of the HIF hydroxylases. *Antioxid. Redox Signal. 12*, 481−501.

(42) Semenza, G. L. (2009) Regulation of Oxygen Homeostasis by Hypoxia-Inducible Factor 1. *Physiology 24*, 97−106.

(43) Simmons, J. M., Muller, T. A., and Hausinger, R. P. (2008) FeII/alpha-ketoglutarate hydroxylases involved in nucleobase, nucleoside, nucleotide, and chromatin metabolism. *Dalton Trans.*, 5132−5142.

(44) Zheng, G., Fu, Y., and He, C. (2014) Nucleic Acid Oxidation in DNA Damage Repair and Epigenetics. *Chem. Rev. 114*, 4602−4620.

(45) Ehrismann, D., Flashman, E., Genn, D. N., Mathioudakis, N., Hewitson, K. S., Ratcliffe, P. J., and Schofield, C. J. (2007) Studies on the activity of the hypoxia-inducible-factor hydroxylases using an oxygen consumption assay. *Biochem. J. 401*, 227−234.

(46) Koivunen, P., Hirsilä, M., Günzler, V., Kivirikko, K. I., and Myllyharju, J. (2004) Catalytic properties of the asparaginyl hydroxylase (FIH) in the oxygen sensing pathway are distinct from those of its prolyl 4-hydroxylases. *J. Biol. Chem. 279*, 9899−9904.

(47) Ryle, M. J., Padmakumar, R., and Hausinger, R. P. (1999) Stopped-flow kinetic analysis of *Escherichia coli* taurine/α-ketoglutarate dioxygenase: Interactions with α-ketoglutarate, taurine, and oxygen. *Biochemistry 38*, 15278−15286.

(48) Fitzpatrick, P. F. (1991) Steady-state kinetic mechanism of rat tyrosine-hydroxylase. *Biochemistry 30*, 3658−3662.

(49) Saam, J., Ivanov, I., Walther, M., Holzhütter, H. G., and Kuhn, H. (2007) Molecular dioxygen enters the active site of 12/15-lipoxygenase via dynamic oxygen access channels. *Proc. Natl. Acad. Sci. U. S. A. 104*, 13319−13324.

(50) Knapp, M. J., and Klinman, J. P. (2003) Kinetic studies of oxygen reactivity in soybean lipoxygenase-1. *Biochemistry 42*, 11466−11475.

(51) Hirsilä, M., Koivunen, P., Günzler, V., Kivirikko, K. I., and Myllyharju, J. (2003) Characterization of the human prolyl 4-hydroxylases that modify the hypoxia-inducible factor. *J. Biol. Chem. 278*, 30772−30780.

(52) Cascella, B., and Mirica, L. M. (2012) Kinetic Analysis of Iron-Dependent Histone Demethylases: α-Ketoglutarate Substrate Inhibition and Potential Relevance to the Regulation of Histone Demethylation in Cancer Cells. *Biochemistry 51*, 8699−8701.

(53) Fielden, E. M., Roberts, P. B., Bray, R. C., Lowe, D. J., Mautner, G. N., Rotilio, G., and Calabres, L. (1974) Mechanism of action of Superoxide-Dismutase from pulse-radiolysis and electron-paramagnetic resonance-evidence that only half active-sites function in catalysis. *Biochem. J. 139*, 49−60.

(54) Rotilio, G., Bray, R. C., and Fielden, E. M. (1972) A pulse radiolysis study of superoxide dismutase. *Biochim. Biophys. Acta, Enzymol. 268*, 605–609.
(55) Hasinoff, B. B. (1984) Kinetics of Carbonic-Anhydrase in Solvents of Increased Viscoisty - A Partially Diffusion-Controlled Reaction. *Arch. Biochem. Biophys. 233*, 676–681.
(56) Pocker, Y., and Janjic, N. (1987) Enyzme-Kinetics in Solvents of Increased Viscosity - Dynamic Aspects of Carbonic-Anhydrase Catalysis. *Biochemistry 26*, 2597–2606.
(57) Perry, J. J. P., Shin, D. S., Getzoff, E. D., and Tainer, J. A. (2010) The structural biochemistry of the superoxide dismutases. *Biochim. Biophys. Acta, Proteins Proteomics 1804*, 245–262.
(58) Tian, G., and Klinman, J. P. (1993) Discrimination between ^{16}O and ^{18}O in Oxygen Binding to the Reversible Oxygen Carriers Hemoglobin, Hemerythrin, and Hemocyanin: A new Probe for Oxygen Binding and Reductive Activation by Proteins. *J. Am. Chem. Soc. 115*, 8891–8897.
(59) Tian, G., Berry, J., and Klinman, J. (1994) Oxygen-18 Kinetic Isotope Effects in the Dopamine β-Monooxygenase Reaction: Evidence for a New Chemical Mechanism in Non-Heme Metallomonooxygenases. *Biochemistry 33*, 226–234.
(60) Roth, J. P. (2007) Advances in studying bioinorganic reaction mechanisms: Isotopic probes of activated oxygen intermediates in metalloenzymes. *Curr. Opin. Chem. Biol. 11*, 142–150.
(61) Stahl, S. S., Francisco, W. a, Merkx, M., Klinman, J. P., and Lippard, S. J. (2001) Oxygen kinetic isotope effects in soluble methane monooxygenase. *J. Biol. Chem. 276*, 4549–4553.
(62) Mirica, L. M., and Klinman, J. P. (2008) The nature of O_2 activation by the ethylene-forming enzyme 1-aminocyclopropane-1-carboxylic acid oxidase. *Proc. Natl. Acad. Sci. U. S. A. 105*, 1814–1819.
(63) Francisco, W. A., Tian, G. C., Fitzpatrick, P. F., and Klinman, J. P. (1998) Oxygen-18 kinetic isotope effect studies of the tyrosine hydroxylase reaction: Evidence of rate limiting oxygen activation. *J. Am. Chem. Soc. 120*, 4057–4062.
(64) Hotopp, J. C. D., and Hausinger, R. P. (2002) Probing the 2,4-dichlorophenoxyacetate/α-ketoglutarate dioxygenase substrate-binding site by site-directed mutagenesis and mechanism-based inactivation. *Biochemistry 41*, 9787–9794.
(65) Thornburg, L. D., Lai, M. T., Wishnok, J. S., and Stubbe, J. (1993) A non-heme iron protein with heme tendencies: An investigation of the substrate specificity of thymine hydroxylase. *Biochemistry 32*, 14023–14033.
(66) Saban, E., Chen, Y. H., Hangasky, J., Taabazuing, C., Holmes, B., and Knapp, M. (2011) The second coordination sphere of FIH controls hydroxylation. *Biochemistry 50*, 4733–4740.
(67) Flagg, S. C., Giri, N., Pektas, S., Maroney, M. J., and Knapp, M. J. (2012) Inverse Solvent Isotope Effects Demonstrate Slow Aquo Release from Hypoxia Inducible Factor-Prolyl Hydroxylase (PHD2). *Biochemistry 51*, 6654–6666.
(68) Tarhonskaya, H., Szöllössi, A., Leung, I. K. H., Bush, J. T., Henry, L., Chowdhury, R., Iqbal, A., Claridge, T. D. W., Schofield, C. J., and Flashman, E. (2014) Studies on Deacetoxycephalosporin C Synthase Support a Consensus Mechanism for 2-Oxoglutarate Dependent Oxygenases. *Biochemistry 53*, 2483–2493.
(69) Sanchez-Fernandez, E. M., Tarhonskaya, H., Al-Qahtani, K., Hopkinson, R. J., McCullagh, J. S., Schofield, C. J., and Flashman, E. (2013) Investigations on the oxygen dependence of a 2-oxoglutarate histone demethylase. *Biochem. J. 449*, 491–496.